Revista EIA, ISSN 1794-1237 / Year XII / Volume 12 / Issue N.24 / July-December 2015 / pp. 119-127
Technical-scientific biannual publication / Universidad EIA, Envigado (Colombia)

REMOTE CONTROL SYSTEM OF A ROBOTIC ARM WITH 4 DEGREES OF FREEDOM USING MACHINE VISION

Germán Darío Buitrago Salazar[1]
✉ Olga Lucía Ramos Sandoval[2]

ABSTRACT

Today, robotic applications are accompanied by machine vision systems, which monitor their activities and allow them to be controlled remotely. This paper presents the design and development of a control system for remote control of a robotic arm with 4 degrees of freedom (DOF) of motion using machine vision. The movements of the manipulator and end effector within the workspace are controlled by a joystick-type device that allows the user to generate the path to follow. To determine the position of the robotic arm, a Kinect sensor and reference figure are used. This figure is placed in the final position in the workspace, which is recognized by a machine vision system. The Kinect sensor estimates the distance between the manipulator and the reference object using an infrared (IR) camera depth map. Testing with the remote control system and the machine vision system demonstrated the method's accuracy for calculating spatial distances using the Kinect sensor with low error in relation to actual measurements of distances within the manipulator's working environment.

KEYWORDS: Robotic Arm, Remote Control, Machine Vision, Kinect.

SISTEMA TELEDIRIGIDO DE UN BRAZO ROBÓTICO DE 4 GRADOS DE LIBERTAD APLICANDO VISIÓN DE MÁQUINA

RESUMEN

Las aplicaciones robóticas están acompañadas por sistemas de visión de máquina que supervisan las actividades que desarrollan y permiten su control teledirigido. En este trabajo se presentan los resultados del diseño y desarrollo de un sistema de control para el movimiento teledirigido de un brazo robótico de 4 grados de libertad (DOF), aplicando visión de máquina. Los movimientos del manipulador y su efector final dentro del espacio de trabajo se controlan con un dispositivo de tipo *joystick*, que permite al usuario generar la trayectoria a seguir. Para determinar la posición del brazo robótico se utiliza un sensor Kinect y una figura de referencia situada en la posición final del espacio de trabajo,

[1] Mechatronics Engineer, Universidad Militar Nueva Granada. Bogotá, Colombia.

[2] Electronic Engineer. Specialist in Electronic Instrumentation. Master of Teleinformática, Universidad Militar Nueva Granada, Mechatronics Engineering Program. Bogotá,. Colombia.

✉ *Correspondence author:* Ramos Sandoval, O.L. (Olga Lucía). Universidad Militar Nueva Granada, Programa de Ingeniería en Mecatrónica. Carrera 11 No. 101-80, Bogotá, Colombia / Tel.: (571) 6500000 ext. 1285.
Email: olga.ramos@unimilitar.edu.co

Paper history:
Paper received: 11-XII-2014 / Approved:
Available online: October 30 2015
Open discussion until November 2016

DOI: http:/dx.doi.org/10.14508/reia.2015.12.24.121-129

la cual se reconoce por un sistema de visión de máquina. Esto permite identificar la distancia estimada del manipulador respecto a la figura de referencia, utilizando el mapa de profundidad de la cámara infrarroja (IR). Las pruebas del sistema teledirigido y del sistema de visión de máquina demostraron la exactitud del método para el cálculo de distancias espaciales utilizando el Kinect, con un error bajo, respecto a las distancias medidas reales dentro del entorno de trabajo del manipulador.

PALABRAS CLAVES: brazo robótico, control teledirigido, visión de máquina, Kinect.

SISTEMA DE CONTROLE REMOTO DE UM BRAÇO ROBÓTICO 4 GRAUS DE LIBERDADE APLICANDO VISÃO DE MÁQUINA

RESUMO

Aplicações robóticas são acompanhados por sistemas de visão de máquina que monitoram suas atividades e permitem o controle remoto. Neste trabalho, são apresentados os resultados do projeto e desenvolvimento de um sistema de controle para o controle remoto de um braço robótico 4 graus de liberdade (DOF) de movimento usando visão de máquina. Os movimentos do manipulador e um efeito final no espaço de trabalho são controladas por um dispositivo do tipo joystick que permite ao utilizador gerar o caminho a seguir. Para determinar a posição do braço robótico e usado um sensor Kinect e uma figura de referência na posição final do espaço de trabalho, o qual é reconhecido por um sistema de visão por máquina. Isto identifica a distância média do manipulador à Figura de referência, utilizando o mapa de profundidade da distância da câmara de infravermelhos (IR). Os testes do Sistema remoto e do sistema de visão de máquina demonstrou a precisão do método para calcular distâncias espaciais utilizando o Kinect, com um baixo erro sobre distâncias medidas reais dentro do ambiente de trabalho do manipulador.

PALAVRAS-CHAVE: Braço robótico, monitoramento remoto, visão de máquina, Kinect**.**

1. INTRODUCTION

Robotic devices have become a fundamental component for performing repetitive and rigorous activities that were previously performed by a worker. To carry out these tasks, manipulators must be controlled such that the movements they make in their environment allow the manipulator's final effector to arrive at a specific objective while avoiding the obstacles it may find in its path. To control these movements, machine vision algorithms are applied which supervise and locate obstacles while a remote control system governs the robot's position.

The main areas in which manipulators have been implemented include surgical and automotive processes. In the automotive area, robotic arms are used on the assembly lines in stamping, the car body workshop, painting, and final assembly, as explained by Michalos et al. (2010). For example, in this latter stage, a camera system was adapted for the manipulator arms to visualize elements and detect anomalies that could affect the quality and proper function of the final product, as explained by Bone & Capson (2013).

In the area of surgery, robotic arms have been implemented thanks to the high precision of their movements during the process and the reduction of recovery times and hospitalization of patients (Lanfranco et al., 2004). Surgical and therapeutic operations that are performed using manipulators show that robots can be used as surgery assistants which are virtually and remotely controlled by a doctor (Muradore et al., 2011). Likewise, these robots are used in patient treatment and

rehabilitation (Ballantyne, 2002). Medical robotics is also used as a mechanism for training personnel for surgeries. In addition, in the educational sphere, they are also used to teach process stages using robots developed for this type of application, such as Zeus, AESOP, and Da Vinci, as is referenced in Valero et al. (2011) and in Pietrabissa et al. (2013).

To control the robot's movements in their workspace and also detect the elements that are within it, machine vision methods have been used with cameras located in the robot's environment. Studies performed with machine vision in robotics include the important contributions of Mapanga & Sampath (2012), who developed a mobile platform controlled by an FPGA (field programmable gate array) for the robotic device to detect obstacles and navigate autonomously. Likewise, the study by Michalos et al. (2012) presents algorithms for machine vision to correct the trajectories of a robotic arm used in parts assembly. This prototype used a stereoscopic vision system to obtain the robot's position based on a map of image disparities.

Other studies related to machine vision systems in robotics include that by Eresen et al. (2012). They simulated the flight system of a quadcopter in a virtual environment while controlling the device's trajectory using the information from the vision system. The main contribution made by Eresen et al. (2012) was presenting a new method for quadcopter navigation in urban environments. Authors like Weichselbaum et al. (2013), Alenya et al. (2014), Einhorn et al. (2011), and Goh & Ponnambalam (2011) developed applications with stereoscopic machine vision for manipulators and mobile robots.

This study presents the results of the design and development of a remotely controlled robotic arm with 4 degrees of freedom based on the machine vision concept. The conventional vision system was replaced by a Kinect since its architecture provides greater precision in the information obtained, it is more robust to image noise, and its price is more economical than that of stereoscopic vision systems. The algorithm proposed for estimating position between the two elements has an error of no more than 2% compared to the elements' real positions. This document is organized into four sections. The second describes the methods and materials used to solve the proposal, the third includes an analysis of the result, and, finally, the last section presents conclusions.

2. METHODS AND MATERIALS

In this study, a robotic arm remote control system was developed. It is composed of a joystick to remotely control the manipulator's movements with regards to the three axes of a reference system located on the robot's base. In addition, to effect rotation of the manipulator's wrist, a fourth movement described by the joystick's rotational axis was used. To supervise the robot's position in the work environment, a Kinect was located within the device's operating distance to capture the image and the depth map of the robot's workspace. By applying a machine vision algorithm, the images are processed and the robot's location is discriminated in relation to a marker located at the end of the robot's trajectory. **Figure 1** shows the process's schematic representation, referencing each of the stages.

Figure 1. Block diagram for the robot manipulator's movement.

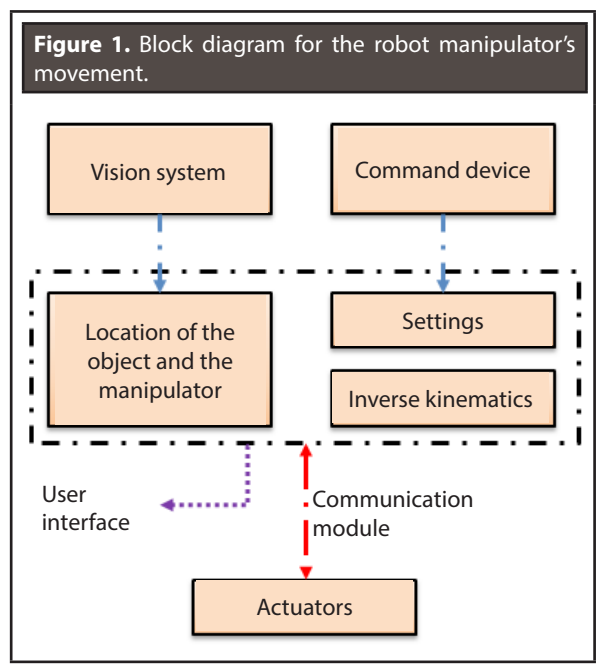

2.1. Physical and kinematic description of the manipulator

As was mentioned above, the remote control system controls the movements of a robotic arm that has three degrees of freedom to position the robot, as well as an additional degree for rotation of the wrist. Each of the manipulator's degrees of freedom has a servomotor, as is shown in the physical structure presented in **Figure 2**.

Figure 2. Schematic model of the 4 DOF manipulator's joints

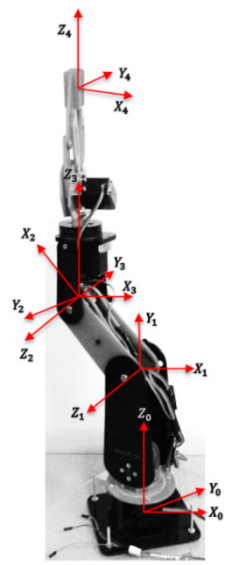

These servomotors have a rotation range of 0° to 135° with a torque of less than 6.91 kg-cm. In accordance with these characteristics, the manipulator's workspace depends on the position in which these motors were situated and the mechanical tolerances, as well as the form and the material. **Table 1** shows the turning range of each of the robot's joints.

To represent the manipulator's kinematic model, the Devanit-Hartenberg design is applied. This design relates the kinematic structure of the chain of links in a robotic arm by taking a reference system for each of the joints (Weber & Darmstadt, 2010). Then the previous orthogonal system (S_{i-1}) is related to the current system (S_i), four transformations represented on a generic matrix are implemented. This matrix can be found in **Equation 1**. The initial system is located on the manipulator's base, as is shown in **Figure 2**. Regarding this beginning point, other systems are laid out based on the Devanit-Hartenberg parameters up to the manipulator's final effector, which, in this case, is a gripper.

TABLE 1. TURNING RANGE OF THE ROBOTIC ARM'S JOINTS

Joint	*Turning range*
θ_1	From 0° to 130°
θ_2	From -65° to 65°
θ_3	From 0° to130°
θ_4	From -20° to 110°

$$A_i^{i-1} = \begin{bmatrix} C\theta_i & -C\alpha_i S\theta_i & S\alpha_i S\theta_i & a_i C\theta_i \\ S\theta_i & C\alpha_i S\theta_i & -S\alpha_i C\theta_i & a_i S\theta_i \\ 0 & S\alpha_i & C\alpha_i & d_i \\ 0 & 0 & 0 & 1 \end{bmatrix} \quad (1)$$

Equation 2 relates each reference system with the robotic arm's base, where n is the number of the manipulator's orthogonal systems, as explained by Abdel-Malek & Othman (1999). **Table 2** includes symbolic representations of the parameters for each of the links, considering that all of the manipulator's joints are rotational.

$$A_n^0 = \prod_{i=1}^{n} A_i^{i-1} \quad (2)$$

TABLE 2. DH PARAMETERS FOR THE 4 DOF MANIPULATOR

Parameters	*θ*	*D*	*a*	*α*
1	θ_1	l_1	0	π/2
2	θ_2	0	l_2	0
3	θ_3	0	0	–π/2
4	θ_4	l_3	0	0

In accordance with **Figure 2**, the Denavit-Hartenberg parameters are obtained and presented in **Table 2**. The goal of obtaining the robot's direct

kinematic model is to find the manipulator's current position in order to then establish the new position to which the robot must move.

After estimating this position, the manipulator's inverse kinematics is found by using the geometric method described by (Weber & Darmstadt, 2010). To do so, the equations are formulated in accordance with the diagram in **Figure 3**, which relates the joint variables to the manipulator's current position and physical structure. For the first joint, the rotation angle is linked to the robot's position presented in **Equation 3**. The values of joints 2 and 3 depend on a mathematical development made beforehand, which is shown in this study from **Equation 4** through **Equation 8**.

$$\theta_1 = Atan2\,(y, x) \tag{3}$$

$$x' = \sqrt{(x^2 + y^2)} \tag{4}$$

$$\alpha = Atan2\,(z - l_1, x') \tag{5}$$

$$h' = \sqrt{x'^2 + (z - l_1)^2} \tag{6}$$

$$\beta = \cos^{-1} \frac{h'^2 + (l_2)^2 - (l_3)^2}{2 * h' * l_2} \tag{7}$$

$$\gamma = \cos^{-1} \frac{(l_3)^2 + (l_2)^2 - h'^2}{2 * l_3 * l_2} \tag{8}$$

Assuming that the robot's position is elbow-up, given that the final effector must reach the object from above in order to achieve a firmer grip, the values of the second and third joints are given by **Equation 9**, where α, β, γ are the internal angles of the robot's structure.

$$\theta_2 = \alpha - \beta \quad \text{y} \quad \theta_3 = \pi - \gamma \tag{9}$$

The fourth degree of freedom is obtained through kinematic decoupling. Matrix R_3^6, which relates the final effector's rotation, is calculated with the rotational component of the manipulator's positional matrix, applied to the first degrees of freedom R_0^3 and to the rotation matrix of a robot with six degrees of freedom R_0^6. The above applies when we assume two of the three Euler angles as constants. **Equation 10** presents the method described above to obtain matrix R_3^6. The values obtained with this method are sent to the manipulator so that it can effect the trajectory described.

$$R_3^6, = (R_0^3)^{-1} * R_0^6 \tag{10}$$

2.2. Monitoring system

Figure 3. Schematic and kinematic diagram of the 4 DOF robot manipulator.

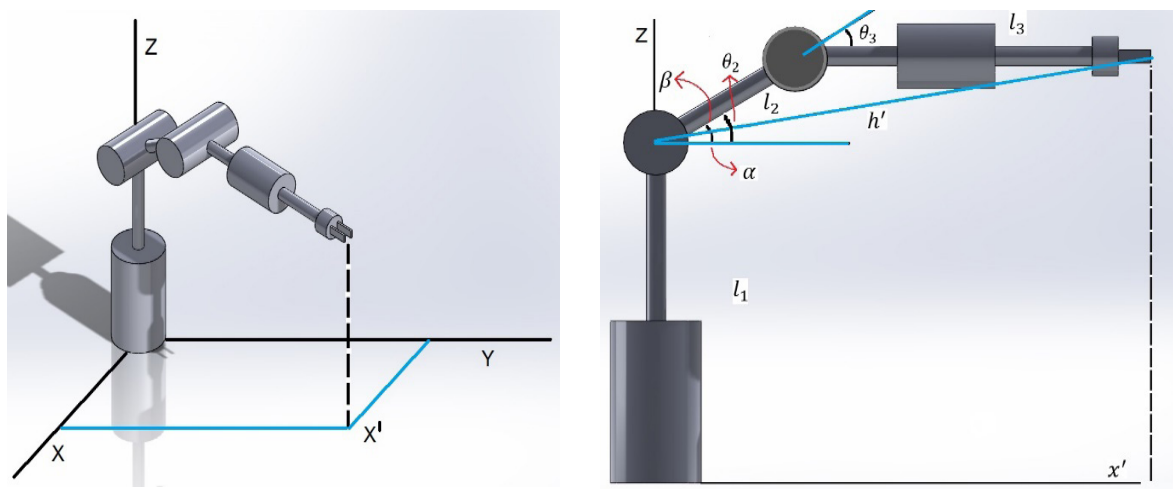

Monitoring systems are mainly used to govern the manipulator's movements without the need for an operator to directly manipulate the robot. In these cases, the manipulator is considered a slave system that imitates the movements made by the operator on a haptic device which, in turn, is the master system (Van Osch, et al., 2014). In this study, a joystick with four axes of movement was used to control the robot's position and thereby effect a trajectory that is the same or similar to that described by the operator with the device.

The first three axes of the joystick move the robotic arm with respect to the orthogonal system S_0, located at the base of the arm, while the last axis controls rotation of the arm's wrist. The system takes information from the joystick and passes through a sigmoid function $f(x)$, delimiting and setting the range of values on a scale of [-1;1] in order to limit the data received from the electronic device. **Figure 4** shows a diagram of the setting process for the joystick, where $f[X_n]$ is the vector with the information from the joystick axes and $f(P_n)$ is the vector with the settings data.

Figure 4. Settings and limits of the joystick values.

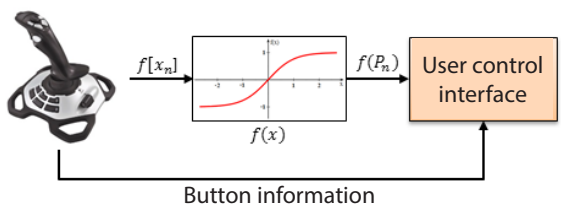

The settings data are multiplied by a conversion factor which depends on the robotic arm's forward speed and the joystick's sampling period. Based on the tests performed, the conversion constant and speed k_v is 2.2. The robotic arm's movement matrix to calculate the manipulator's new position is represented by **Equation 11**, which shows a point-to-point sequence to follow the manipulator's trajectories.

$$\begin{bmatrix} x_i \\ y_i \\ z_i \\ \psi_i \end{bmatrix} = \begin{bmatrix} x_{i-1} \\ y_{i-1} \\ z_{i-1} \\ \psi_{i-1} \end{bmatrix} + k_v \begin{bmatrix} f(P_x) \\ f(P_y) \\ f(P_z) \\ f(P_\psi) \end{bmatrix} \quad (11)$$

2.3. Machine vision

The machine vision system's physical structure is composed of two markers with measurements known by the user and a Kinect device. The sensor, which is programmed with an SDK in C#, has an RGB camera to capture the images and videos, as well as an infrared (IR) sensor that perceives the depths of the environment with a point cloud. The first marker is located at the final position of the trajectory, while the second marker is located on the manipulator. The Kinect is located 80cm away from the closest object within the IR sensor's work range. This distance is within the device's workspace. To evaluate the manipulator's location with regards to the reference object, the regions with the position of the reference figure and the robotic arm are extracted from the RGB image and the depth map, using a bilateral filter. This filter, established using **Equation 12**, relates and combines the information of each of the pixels in the spatial domain image (Gupta & Jing, 2012), separating the color component of the markers from said image according to the size of the vicinity established by the radius and the Gaussian functions of Euclidian distance that can be found in **Equations 13** and **14**.

$$k(x) = \sum_{y \in \Omega_x} f_s(x, y)\, g_r\left(I(x), I(y)\right) \quad (12)$$

$$f_s(x, y) = \exp\left(\frac{-\|x - y\|_2^2}{2\sigma_s^2}\right) \quad (13)$$

$$g_r(u, v) = \exp\left(\frac{-\|u - v\|_2^2}{2\sigma_r^2}\right) \quad (14)$$

The problem proposed in this study is to obtain the real distance between the manipulator and a second object, taking as a basis the position of these elements from the image captured by the Kinect and the space between the camera and the

markers. To do so, we begin with the expressions to calculate the distance over an epipolar plane described in (Lim et al., 2013) and the geometric and architectural representation of the machine vision system using the Kinect, as can be seen in **Figure 5**.

Figure 5. Diagram of the machine vision system using Kinect

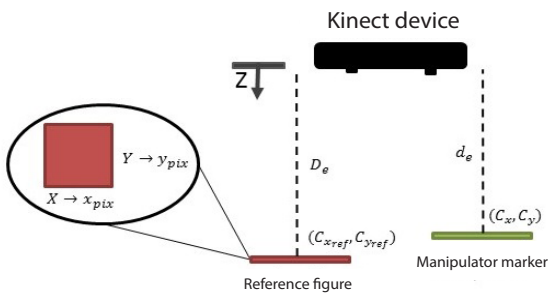

Based on the above, **Equation 15** is proposed, where (C_x, C_y) is the centroid of the region extracted from the image with the manipulator's position; (C_{xref}, C_{yref}) is the centroid of the region of the image with the reference figure; the variables r_x and r_y correspond to the ratio between the size in pixels of the reference figure (x_{pix}, y_{pix}) and the real size of the object (x, y). The distance between the camera and the manipulator's final effector is given by D_e, while the distance between the camera and the reference object is represented by d_e. Likewise, within this type of system, we must consider the camera's intrinsic properties (Sirisantisamrid et al., 2008; Malis, 2001), for which the constants k_x and k_y are added to the equation.

$$\begin{bmatrix} d_x \\ d_y \\ d_z \end{bmatrix} = \begin{bmatrix} \left| C_x - \frac{C_{xref} * D_e}{d_e} \right| * k_x * r_x \\ \left| C_y - \frac{C_{yref} * D_e}{d_e} \right| * k_y * r_y \\ D_e - d_e \end{bmatrix} \quad (15)$$

3. RESULTS

So that the user can interact with the robotic device, an interface was designed to perform two tasks. The first task is processing the video, which detects, in real time, the reference figure (the light blue rectangle in **Figure 6**) and the marker located on the robotic arm's work tool (the green rectangle in **Figure 6**). In this process, the user observes the robot's movements from a remote work station while the distance between the elements is shown on the screen. The second programmed task is the supervision of the robotic device's movement according to the wait time between frames in the video. These tasks are carried out in parallel, using the machine vision and trajectory monitoring systems described above.

Figure 6. Result of the video processing system.

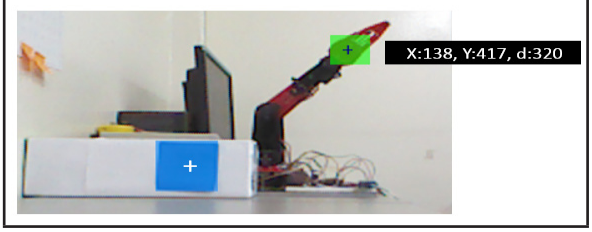

The result of this process can be observed in **Figure 7** with the graphs of the positions of the robotic arm and the final point of the trajectory, where the manipulator's trajectory error decreases as the device approaches the final point such that it tends toward zero. When the machine vision algorithm is used to compare the distance values obtained to the real measurements between the manipulator and the final position, it is observed that the absolute error is less than 10% when the manipulator approaches the end of the trajectory. This error is produced by the Kinect camera's resolution and the vision system's sensitivity to detect the corresponding colors.

4. CONCLUSIONS

In the project's development, a machine vision system was proposed based on the information collected by the Kinect sensor to establish the manipulator's distance in relation to a reference system located at the final position of the trajectory. The feedback from the position corrected, in real time, the trajec-

Figure 7. A) Manipulator's movement on the x-axis. B) Manipulator's movement on the y-axis. C) Manipulator's movement on the z-axis.

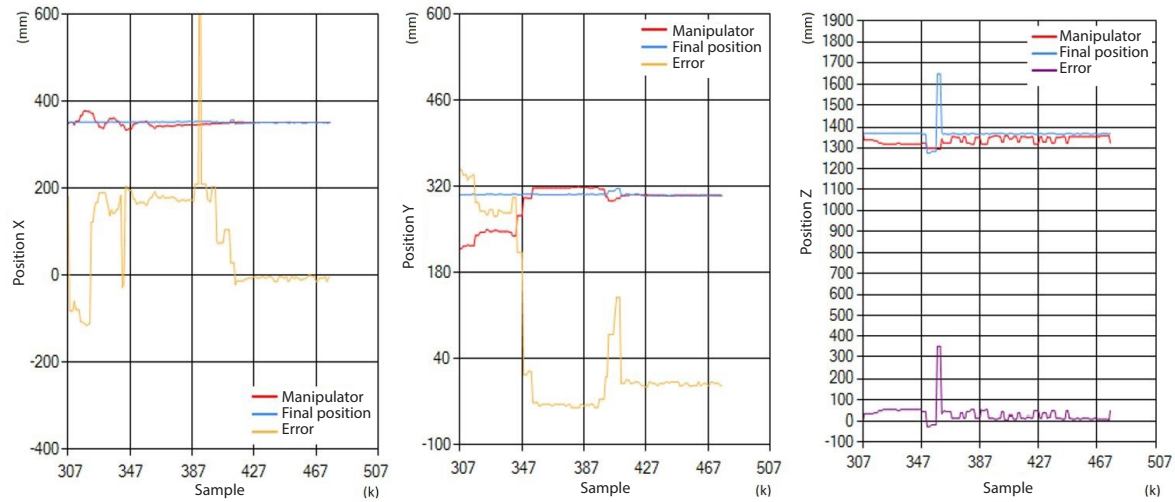

tory described by the joystick device, thereby reducing error as the manipulator approached the final position and validating the machine vision system's effectiveness.

Likewise, when the results of real distance are compared to the estimated distance for each of the tests performed, the errors were low, which implies that the exactness of the machine vision algorithm combined with the Kinect device has a high level and, therefore, the machine vision system can be adapted to industrial processes in which it is necessary to have a trajectory control as close as possible to that described.

The errors described above are mainly caused by the configuration of the Kinect device's parameters, the image processing times, and the sensitivity of the artificial vision system for recognizing patterns. The error caused by the parameter configuration is due to the fact that the camera's resolution is not the same as that of the IR sensor. Therefore, the camera was configured to a lower resolution and image quality was lost. The error due to image processing times is caused by the amount of machine resources needed to process these images, which produces an increase in the capture time and the loss of the real position at which the manipulator is located. Finally, the error in pattern recognition is due to the similarity in tones between the colors to be recognized, such that they are confused. To compensate for this error, the Euclidian filter radius for neighboring pixels was modified, thereby allowing the vision system to be more robust.

REFERENCES

Abdel-Malek, K. y Othman, S. (1999). Multiple Sweeping Using the Denavit-Hartenberg Representation Method. *Computer-Aided Design*, 31 (9), August, pp. 567-583.

Alenya, G.; Foix, S. y Torras, C. (2014). ToF Cameras for Active Vision in Robotics. *Sensors and Actuators A: Physical*, 218, pp. 10-22.

Ballantyne, G. H. (2002). Robotic Surgery, Telerobotic Surgery, Telepresence, and Telementoring. *Surgical Endoscopy and Other Intervetional Techniques*, 16 (10), pp. 1389-1402.

Bone, G. M. y Capson, D. (2013). Vision-Guided Fixtureless Assembly of Automotive Components. *Robotic and computer Integrated Manufacturing*, 19, pp. 79-87.

Einhorn, E.; Schröter, C. y Gross, H. M. (2011). Attention-Driven Monocular Scene Reconstruction for Obstacle Detection. *Robot Navigation and Map Building. Robotics and Autonomous Systems*, May, 59 (5), pp. 269-309.

Eresen, A.; Imamoglu, N. y Önder, M. (2012). Autonomous Quadrotor Flight with Vision-Based Obstacle Avoidance in Virtual Environment. *Expert Systems with Applications*, Enero, 39 (1), January, pp. 894-905.

Goh, S. C. y Ponnambalam, S. G. (2011). Obstacle Avoidance Control of Redundant Robots Using Variants of Particle Swarm Optimization. *Robotics and Computer-Integrated Manufacturing*, Abril, 28 (2), April, pp. 147-153.

Gupta, M. D. y Jing, X. (2012). Bi-affinity Filter: Abilateral Type Filter for Color Images. *Trends and Topics in Computer Vision*, Volumen 6554, pp. 27-40.

Lanfranco, A., *et al*. (2004). Robotic Surgery. *Annals of Surgery*, 239 (1), January, pp. 14-21.

Lim, K. B.; Keen, W. L. y Wang, D. (2013). Virtual Camera Calibration and Stereo Correspondence of Single-Lens Bi-prism Stereovision System Using Geometrical Approach. *Journal Image Communication*, 28 (9), October, pp. 1059-1071.

Malis, E. (2001). Visual Servoing Invariant to Changes in Camera-Intrisic Parameters. [pdf] Available at: http://citeseerx.ist.psu.edu/viewdoc/download?doi=10.1.1.58.9499&rep=rep1&type=pdf

Mapanga, K. y Sampath-Kumar, V.R. (2012). Machine Vision for Intelligent Semi-Autonomous Transport (MV-iSAT). *Procedia Engineering*, 41, pp. 395-404.

Michalos, G. *et al*. (2012). Robot Path Correction Using Stereo Vision System. *Procedia CIRP*, Volumen 3, pp. 352-357.

Michalos, G. *et al*. (2010). Automotive Assembly Technologies Review: Challenges and Outlook for a Flexible and Adaptive Approach. *CIRP Journal of Manufacturing Science and Technology*, 2 (2), January, pp. 81-91.

Muradore, R. *et al*, (2011). Robotic Surgery. *IEEE Robotics & Automation Magazine*, September, pp. 24-32.

Pietrabissa, A., *et al*. (2013). Robotic Surgery: Current Controversies and Future Expectations. *Cirugia Española*, 91(2), February, pp. 67-71.

Sirisantisamrid, K., *et al*. (2008). An Influential Principal Point on Camera Parameters. *Control, Automation and Systems, 2008. ICCAS 2008. International Conference on., October,* pp. 2797-2800.

Valero, R. *et al*. (2011). Robotic Surgery: History and Teaching Impact. *Actas Urológicas Españolas*, 35 (9), October, pp. 540-545.

Van Osch, M. *et al*. (2014). Tele-Operated Service Robots: ROSE. *Automation in Construction*, 39 (1), April, pp. 152-160.

Weber, W. y Darmstadt, H. (2010). Automatic Generation of the Denavit-Hatenberg Convention. *Robotik*, pp. 235-241.

Weichselbaum, J., et al. (2013). Accurate 3D-Vision-Based Obstacle Detection for an Autonomous Train. *Computers in Industry*, December, 64 (9), December, pp. 1209-1220.

TO REFERENCE THIS ARTICLE / PARA CITAR ESTE ARTÍCULO / PARA CITAR ESTE ARTIGO /

Buitrago Salazar, G.D.; Ramos Sandoval, O.L. (2015). Remote Control System of a Robotic Arm with 4 Degrees of Freedom Using Machine Vision. *Revista EIA*, 12(24), July-December, pp. 119-127. [Online]. Available on: DOI: http:/dx.doi.org/10.14508/reia.2015.12.24.121-129